Title
Multi-dimensional Point Process Models for Evaluating a Wildfire Hazard Index

Authors
Peng, Roger D.
Schoenberg, Frederic P.
Woods, James

Publication Date
2003

Multi-dimensional Point Process Models for Evaluating a Wildfire Hazard Index

Roger D. Peng Frederic Paik Schoenberg James Woods

Author's footnote: Roger D. Peng (rpeng@stat.ucla.edu) is a Graduate Student, Department of Statistics, University of California, Los Angeles CA 90095; Frederic Paik Schoenberg is Assistant Professor, Department of Statistics, University of California, Los Angeles CA 90095; and James Woods is GIS Lab Manager and Instructor, Department of Geography, California State University, Long Beach, CA 90840. This work is part of the first author's Ph.D. dissertation from the University of California, Los Angeles. The material is based upon work supported by the National Science Foundation under Grant No. 9978318. The authors thank Larry Bradshaw at the USDA Forest Service for providing the weather station data as well as LADPW and LACFD (esp. Mike Takeshita and Frank Vidales) for generously sharing their data and expertise.

Abstract

The Burning Index (BI) is part of the U.S. National Fire Danger Rating System and is widely used as a tool for fire management and hazard assessment. While the usage of such indices is widespread, assessment of these indices in their respective regions of application is rare. We evaluate the effectiveness of the BI for predicting wildfire occurrences in Los Angeles County, California using space-time point process models. The models are based on an additive decomposition of the conditional intensity, with separate terms to describe spatial and seasonal variability as well as contributions from the BI. The models are fit to wildfire and BI data from the years 1976–2000 using a combination of nonparametric kernel smoothing methods and parametric maximum likelihood. In addition to using AIC to compare competing models, new multi-dimensional residual methods based on approximate random thinning are employed to detect departures from the models and to ascertain the precise contribution of the BI to predicting wildfire occurrence. We find that while the BI appears to have a positive impact on wildfire prediction, the contribution is relatively small after taking into account natural seasonal and spatial variation. In particular, the BI does not appear to take into account increased activity during the years 1979–1981 and can overpredict during the early months of the year.

Keywords: Point process residual analysis; Random thinning; Random rescaling; Conditional intensity model; Model evaluation; Wildfire risk

1 Introduction

Fire departments all over the world often use numerical indices to aid in wildfire management. These indices are designed to summarize local meteorological and fuel information and provide an estimate of the current risk of fire. The many index systems in use today have been developed both by national governments and various independent fire researchers.

Some well-known indices in the United States include the Keetch-Byram Index, Palmer Drought Severity Index, and the Fosberg Fire Weather Index. The variety of different index systems in some ways reflects the diversity of landscapes and wildfire settings in the United States and the rest of the world.

The Burning Index is part of the U.S. National Fire-Danger Rating System, a collection of numerical indices designed to be used for fire planning and management. In Los Angeles County, California, the fire department uses the Burning Index for creating short-term wildfire hazard maps of the County. These maps help managers make decisions involving the allocation of resources and the coordination of various presuppression activities.

While the Burning Index is already in common use (by Los Angeles and other fire departments), there have been relatively few attempts to assess the Index's performance in predicting wildfires. In the general area of index evaluation, there has been some work in evaluating elements of the U.S. system (e.g. Haines et al., 1983), various national (non-U.S.) systems (Viegas et al., 1999), and in using indices for prediction (Westerling et al., 2000). However, the Burning Index's ability to adapt to particular regions such as Los Angeles County has yet to be fully scrutinized. Mandallaz and Ye (1997) have noted that in general, wildfire hazard indices are developed on the basis of experience in a given area. Therefore, one must take caution when adapting indices to other areas.

The aim of this paper is to evaluate the performance of the Burning Index in predicting wildfires in Los Angeles County. Our approach is to evaluate the best-fitting conditional intensity model both with and without the BI and other information, in order to determine not only the optimal use of the BI in point process prediction, but also to assess the increase in prediction performance using the BI as compared to other information. The various conditional intensity models are compared using the Akaike Information Criterion (AIC) as well as multi-dimensional residual analysis methods based on approximate random

thinning. While the AIC proves to be useful for finding the best model in set of possibilities, residual analysis can identify specific areas where the performance is poor and suggest directions for improvement.

In the sections to follow we briefly describe the U.S. National Fire-Danger Rating System and provide a summary of the data used for this analysis. We then outline the point process methodology used for evaluating the performance of the Burning Index and discuss the method of multi-dimensional residual analysis employed for assessing the performance. Finally, the results of applying these methods to the wildfire data from Los Angeles County, California are discussed.

2 A Brief Summary of the National Fire-Danger Rating System

The U.S. National Fire-Danger Rating System (NFDRS) was developed by the U.S. Department of Agriculture Forest Service in 1972 (Deeming et al., 1972) and was revised in 1978 (Deeming et al., 1977; Bradshaw et al., 1983). Since then there have been some adjustments (see e.g. Burgan, 1988). The NFDRS actually consists of multiple components which can be combined in various ways. The three core components are the Ignition, Spread and Energy Release Components. Using these components, three different indices can be computed: the Lightning-caused Fire Occurrence Index, the Man-caused Fire Occurrence Index, and the Burning Index. Furthermore, these three indices can be combined into an overall Fire Load Index. Although this is a "national" system, there are many parameters which can be calibrated to adapt the system to local environments. In particular, a fire manager must choose a *fuel model* (from a set of 20 available models) which corresponds

to the available fuel in the region. The fuel model is then incorporated into the index computations to produce an index for a specific region (Bradshaw et al., 1983).

2.1 Computing the Burning Index

Since the Los Angeles County Fire Department only uses the Burning Index portion of the NFDRS for hazard assessment, we omit the details of the other indices here. The Burning Index (BI) is computed from the Spread Component (SC) and the Energy Release Component (ERC) of the NFDRS. Both the SC and the ERC are computed using meterological and fuel data gathered by Remote Automatic Weather Stations (RAWS). The RAWS collect data on precipitation, wind direction, wind speed, air temperature, fuel temperature, and relative humidity (Warren and Vance, 1981). The RAWS also collect data relevant to station maintenance which are not used in computing the BI. Collection of the data occurs at approximately 1:00 PM when conditions for fire are considered to be most severe. Once collected, the data are transmitted via satellite to a central station for archiving and can be downloaded by fire managers.

The SC is simply the unmodified fire spread model of Rothermel (1972). Rothermel's spread model is a function of wind, slope, and various fuel properties such as the surface area to volume ratio, heat of ignition, and others. The ERC is a function of the loading-weighted reaction intensity and the surface area to volume ratio of the fuel bed. Given values for the SC and the ERC, the BI itself is computed via the relation (Bradshaw et al., 1983)

$$\mathrm{BI} = 10 \times 0.45 \times \left[\left(\frac{\mathrm{SC}}{60} \right) (25 \times \mathrm{ERC}) \right]^{0.46}.$$

The designers of the BI intended for it to be interpreted as 10 times the *flame length* (Byram, 1959; Albini, 1976). That is, if one observes a value X of the BI, then one might expect to see $X/10$ foot flames, if a fire occurs (note that the BI itself is dimensionless). Given the

flame length interpretation, the BI is sometimes used as a measure of the "containability" of a fire.

3 Data

For the our analysis of the BI we obtained wildfire data for Los Angeles County and meteorological data for computing the BI. In this section we describe the data and explore some of their properties.

3.1 Wildfire Data

The wildfire data were collected and compiled by various agencies, including the Los Angeles County Fire Department (LACFD), the Los Angeles County Department of Public Works, the Santa Monica Mountains National Recreation Area, the Ventura County Fire Department, and the California Department of Forestry and Fire Protection. The full dataset consists of times (to the nearest day) and locations of wildfires between January 1878 and September 2000. LACFD officials have noted that before 1950 (approximately), only fires larger than 100 acres were mapped. After 1950, the Department began mapping some fires as small as 1 acre. Based on work in Schoenberg et al. (2003a) and Schoenberg et al. (2003b), as well as Fire Department guidance, a lower threshold of 10 acres was chosen for determining which fires to include in the analysis. Finally, since BI data was only available since 1976, fires prior to that year were excluded. These criteria produced a catalog of 592 fires between 1976 and 2000 for use in the analysis.

Figure 1 shows the spatial distribution of wildfires larger than 10 acres in LA County for 1976–2000. The locations are represented with a (scaled) state-plane coordinate system using the NAD 83 datum. For our dataset one spatial unit corresponds to approximately 18.9 miles. Much of the wildfire activity occurs in the eastern and northern parts of the

County. These regions consist of the Angeles National Forest and parts of the Los Padres National Forest. One exception to this general pattern is the Santa Monica Mountains area (the protrusion in the western part of the County), which has also experienced significant wildfire activity in the 25 year period. Figure 2 shows the times and areas burned for each of the fires in the dataset. The times are measured to the nearest day and the area burned for each fire is in acres. In the years 1979–1981, there appears to be some intense temporal clustering of points, especially for fires in the 50–500 acre range. This is a feature of the data to which we will return in Section 5.

3.2 Meteorological and Burning Index Data

Daily meteorological observations for eight RAWS around Los Angeles County were obtained from the USDA Forest Service. The locations for each of the RAWS are shown in Figure 1. For each of the 8 stations, daily values of the BI were then computed using the FireFamily Plus software (freely available from the Forest Service). It should be noted that not all of the stations contained data covering the entire 25 year span from 1976 to 2000. Of the eight stations, only Stations 3 and 4 had data going back to 1976. However, each of the stations had at least five years of daily data.

The data from each of the RAWS exhibit the natural seasonal patterns for weather in Los Angeles County. Figure 3 shows the average computed BI value (averaged over all available years) for each day in the year. There is an increase in the BI from February through August and September and then a steady decrease through December and January. Station 1 did not have any observations for the months of January, February, and March. However, in the entire 25 year interval of interest, only 10 fires ever occurred in the months of January, February, and March, representing less than 2% of the total number of fires. Therefore, for Station 1, the BI values were set to zero during that three month span. The

other stations also contained days with missing weather records. In this situation we filled in a missing BI value on a given day with the average of that day across all the other available years. The percentages of missing data are shown in Table 1 for the off-season (January–April), the fire season (May–December) and overall. In Section 6 we will discuss the possible impacts of missing data on the analysis.

4 Methodology

In evaluating the BI our approach involves considering the times and centroids of each fire as points of a space-time point process. We consider a space-time point process N to be a σ-finite counting measure on the spatial-temporal domain $\mathcal{S} \times \mathbb{R}^+$. Given a Borel set $B \subset \mathcal{S} \times \mathbb{R}^+$, $N(B)$ is the number of points in B. Let $\mathcal{F}_t$ be a filtration, that is, an increasing family of σ-algebras, and take $N(S \times [0,t])$ to be $\mathcal{F}_t$-adapted for each Borel set $S \in \mathcal{S}$. In applications, $\mathcal{S}$ is usually taken to be a subset of $\mathbb{R}^2$.

The conditional intensity function of a point process is defined as a non-negative $\mathcal{F}_t$-predictable process $\lambda(t,x,y)$ such that for each Borel set $S \in \mathcal{S}$

$$N(S \times [0,t]) - \iint_S \int_0^t \lambda(t,x,y)\, dtdxdy$$

is an $\mathcal{F}_t$-martingale. It is well known that for point processes with simple ground processes (i.e. with no two points at exactly the same time), the conditional intensity (when it exists) uniquely characterizes all of the finite-dimensional distributions of the point process. For a more thorough treatment of conditional intensities we refer the reader to Jacod (1975), Brémaud (1981), and Daley and Vere-Jones (2003). Intuitively, one may consider the conditional intensity function as describing the conditional expected rate of occurrence of points at time t and location (x,y). In particular, a version of the conditional intensity may be

given by the process

$$\lambda(t,x,y) = \lim_{\Delta t \Delta x \Delta y \downarrow 0} \frac{\mathbb{E}\left[N((t,t+\Delta t)\times(x,x+\Delta x)\times(y,y+\Delta y)) \mid \mathcal{F}_t\right]}{\Delta t \Delta x \Delta y}$$

for $(t,x,y) \in S$, provided the limit exists (Schoenberg et al., 2002).

In prescribing a model for λ, we use a spatial background component $m(x,y)$ which takes into account the spatial inhomogeneity of the wildfire occurrences. This component can be thought of as incorporating previous knowledge about where wildfires are more or less likely to occur. For example, it would be undesirable for the model to predict a wildfire occurrence in downtown Los Angeles. For this component a simple two-dimensional kernel smoother is used,

$$m(x,y) = \frac{1}{n_0} \sum_{j=1}^{n_0} K\left(\frac{x - x_{0j}}{\phi_x}\right) K\left(\frac{y - y_{0j}}{\phi_y}\right).$$

where K is a suitable kernel function. Similar approaches using kernel smoothing have been taken in the area of seismology (see e.g. Choi and Hall, 1998; Zhuang et al., 2002). In estimating the spatial background $m(x,y)$, the smoother is not computed using the 1976–2000 data. Rather the spatial locations of the wildfires occurring before 1976 are smoothed. Here, n_0 is the number of wildfires in the full dataset occurring before 1976 and (x_{0j}, y_{0j}) represents the spatial coordinates of the jth fire in that subset.

A seasonal component $S(t)$ is used to describe the overall seasonal variation of the wildfire activity. Here we smooth the times within each year of the pre-1976 fires,

$$S(t) = \frac{1}{n_0} \sum_{j=1}^{n_0} K\left(\frac{t^* - t^*_{0j}}{\phi_{\text{seas}}}\right)$$

where t^* indicates the time since the beginning of the year and t^*_{0j} is the time since the beginning of the year of the jth wildfire occurrence before 1976.

Finally, a BI component $B(t,x,y)$ describes, for an arbitrary point (t,x,y), the contribution to the conditional intensity from the values of the BI at each station. Since the

BI values are only observed at fixed locations in the County, some form of interpolation is required to compute values at other locations. The BI component is of the form

$$B(t,x,y) = \frac{1}{C}\sum_{s\in S_t}\left\{\gamma_s K\left(\frac{x-x_s}{\beta_s}\right)K\left(\frac{y-y_s}{\beta_s}\right)\mathrm{BI}(t,s)\right\}$$

where $\mathrm{BI}(t,s)$ is the the BI value recorded at time t from the sth, (x_s, y_s) represents the location of the sth station, and S_t is the index set of stations in use at time t. The normalization constant C is simply the sum of the kernel weights,

$$C = \sum_{s\in S_t} K\left(\frac{x-x_s}{\beta_s}\right)K\left(\frac{y-y_s}{\beta_s}\right).$$

For each of the three components, the kernel function used is the normal density,

$$K(z) = \frac{1}{\sqrt{2\pi}}\exp\left(-z^2/2\right).$$

One may consider as a basis of comparison simple baseline models such as a homogeneous Poisson model

$$\lambda^H(t,x,y) = \mu \tag{1}$$

and the following,

$$\lambda^0(t,x,y) = \nu\, m(x,y) + \alpha\, S(t). \tag{2}$$

where μ, ν and α are parameters to be estimated. The model in (2) does not include any information from the BI and serves as a model against which we can compare models incorporating BI information from each station. We take

$$\lambda(t,x,y) = \nu\, m(x,y) + \alpha\, S(t) + B(t,x,y) \tag{3}$$

as our "BI model" and inspect the usefulness of the BI by assessing the performance of both λ and λ^0.

4.1 Parameter Estimation

All parameters for each of the models were estimated by maximizing the log-likelihood function

$$\ell(\boldsymbol{\theta}) = \sum_{i=1}^{n} \log \lambda(t_i, x_i, y_i; \boldsymbol{\theta}) - \int_{T_1}^{T_2} \iint_{S} \lambda(t, x, y; \boldsymbol{\theta})\, dxdydt$$

where $\boldsymbol{\theta}$ is a vector of free parameters and n is the total number of events (t_i, x_i, y_i) in the dataset, observed in the time interval $[T_1, T_2]$ over the area S. The parameters to be estimated are ν, α, ϕ_x, ϕ_y, and ϕ_{seas}, as well as the BI parameters γ_s and β_s $(s = 1, \ldots, 8)$.

Under fairly general conditions, the maximum likelihood estimates (MLEs) have been shown to be consistent and asymptotically normal (Ogata, 1978; Rathbun and Cressie, 1994; Rathbun, 1996). For the homogeneous Poisson model, the MLE can be written in closed form and is simply

$$\lambda^H(t, x, y; \hat{\boldsymbol{\theta}}) = \hat{\mu} = \frac{n}{\|S\|(T_2 - T_1)}$$

where $\|S\|$ is the total area of the observation region. For models other than the homogeneous Poisson model, one must resort to numerical optimization methods for estimating the parameters.

When optimizing the log-likelihood some restrictions had to be placed on the parameters in order to maintain a positive conditional intensity function and numerical stability of the optimization procedure. We restricted the parameters in each of the models to be positive. In addition, the bandwidth parameters in the spatial and seasonal components were bounded away from zero. The inclusion of the β_s parameters in the BI component increased the complexity of the likelihood surface considerably and created some difficulty with the numerical optimization. Ogata et al. (1982) and Ogata and Akaike (1982) handled a similar problem with a single bandwidth parameter by restricting that parameter to a finite grid and repeating the maximum likelihood procedure for each value of the bandwidth

parameter on the grid. Unfortunately for our situation, with 8 separate parameters (one for each weather station), constructing a reasonable grid over which to optimize the log-likelihood was computationally infeasible. Rather, we chose to restrict the β_s parameters to be less than 3.0 spatial units (about 56 miles). This upper limit seemed reasonable in the sense that a particular weather station should not have influence over points with a distance of over 50 miles from the station (see e.g. Haines et al., 1983).

4.2 Residual Analysis via Approximate Random Thinning

Various methods for constructing a residual point process have been proposed based on random rescaling (Merzbach and Nualart, 1986; Nair, 1990; Schoenberg, 1999) and random thinning (Schoenberg, 2003). One-dimensional residual analysis via the rescaling method has been successfully applied in a wide variety of applications (e.g. Berman, 1983; Ogata, 1988; Diggle, 1990; Rathbun, 1993; Brown et al., 2001). However, rescaling can be awkward to use for multi-dimensional residual analysis. In practice, when the points are rescaled (especially along spatial dimensions) the domain of observation is also rescaled and can become uninterpretable or irregular (see Schoenberg, 1997, for examples). In particular, many standard tests for homogeneity can be severely biased if the domain is very irregular (Diggle, 1983). Schoenberg (2003) proposed a method based on approximate random thinning of the observed points. This method has the advantage that the resulting residual process lies in the same domain as the observed point process.

The algorithm for approximate random thinning is conceptually straightforward and easy to implement:

1. Choose a positive integer K such that $K < n$, where n is the total number of points observed.

2. For $i = 1, \ldots, n$, compute

$$p_i = \frac{1/\lambda(t_i, x_i, y_i; \hat{\boldsymbol{\theta}})}{\sum_{j=1}^{n} 1/\lambda(t_j, x_j, y_j; \hat{\boldsymbol{\theta}})}$$

   where $\lambda_{\hat{\boldsymbol{\theta}}}(t, x, y)$ is the estimated conditional intensity function.

3. Using probability weights $p_1, \ldots, p_n$, take a subsample of size K from the original points $\{(t_i, x_i, y_i)\}$ to produce points $\{(t_j^*, x_j^*, y_j^*)\}$ $(j = 1, \ldots, K)$.

4. The points $(t_1^*, x_1^*, y_1^*), \ldots, (t_K^*, x_K^*, y_K^*)$ form the residual process.

The algorithm attempts to "thin out" points in areas with high intensity and retain points in areas of low intensity. One may choose to repeat the algorithm many times to produce multiple random realizations of approximate thinned residuals.

If K is chosen to be relatively small compared to n and the fitted conditional intensity approximates closely the true conditional intensity governing the point process, then the residual process should resemble a homogeneous Poisson process with rate $K/(\|S\|(T_2 - T_1))$ over the original domain of the process. The approximate nature of the residuals is in contrast with residual methods based on ordinary random thinning where the residual process is exactly homogeneous Poisson if the model is known. These methods use modified versions of the algorithms of Lewis and Shedler (1979) and Ogata (1981). With approximate random thinning, even if the true model is known, the residual process will not be exactly homogeneous Poisson. However, as noted in Schoenberg (2003), ordinary random thinning is not possible with some models where the minimum of the conditional intensity is very close to zero.

The primary advantage of generating a residual process is that the problem of evaluating the fit of a possibly complex model is reduced to examining whether the residual process is similar to a homogeneous Poisson process, a task for which there are many tests and

diagnostics. Once the residuals have been produced one can simply display them in residual plots or compute summary statistics. The summary statistics can be compared with corresponding quantities from a homogeneous Poisson process. For example, one may wish to test for residual clustering or inhibition via a statistic such as the K-function (Ripley, 1981). In Section 5.1.1 we use a spatial-temporal version of the K-function to quantify the clustering in the approximate thinned residual process.

5 Application to Wildfire and Burning Index Data

Each of the models in (1)–(3) were fit to the data by maximum likelihood. The maximum likelihood estimates for the parameters in the spatial and seasonal components of each of the models are shown in Table 2. The homogeneous Poisson model is described in (1) and the "Spatial+Seasonal" model is from (2). The model denoted as "BI model" is described in (3) and incorporates data from the eight weather stations.

The estimate for $\hat{\mu}$ in the homogeneous Poisson model (shown in Table 2) was 0.0041 events/(spatial unit^2 $\times$ day), indicating an average of 24 fires per year in the County. The bandwidth parameters for the spatial background component of the Spatial+Seasonal model were estimated as $\hat{\phi}_x = 0.0440$ spatial units (0.83 miles) in the x direction (east-west) and $\hat{\phi}_y = 0.0259$ spatial units (0.49 miles) in the y direction (north-south) for the Spatial+Seasonal model. For the best-fitting BI model, the estimates for the spatial bandwidth parameters were similar, although somewhat smaller. The estimate for the bandwidth parameter of the seasonal component was approximately 8 days for both models. The BI model gives less weight to both the spatial background and the seasonal component, as is evident from the smaller estimates for both ν and α. The estimates of the station multiplier coefficients ($\gamma_s, s = 1, \ldots, 8$) and the β_s's in the BI component are shown in Table 3. Many of the coefficients are estimated to be zero, likely resulting from the high correlation of the

BI values between different stations. The stations receiving non-zero weight are Stations 1, 4, 5, and 7.

To compare the overall fit of each of the models we used the Akaike Information Criterion (AIC). Not unexpectedly, there is a dramatic decrease in AIC from 7693.9 for the homogeneous Poisson model to 6741.1 for the Spatial+Seasonal model. The addition of the weather stations in the BI model decreased the AIC to 6704.6. The decrease in AIC between the Spatial+Seasonal and BI model indicates that the BI component is in fact improving the fit of the model, even with the addition of 16 parameters (2 for each station). However, the relative decrease in AIC is somewhat smaller than the decrease between the homogeneous Poisson and the Spatial+Seasonal models, suggesting that the impact of the BI component (if any) is more subtle.

One can test the significance of the added BI component with a likelihood ratio test. The likelihood ratio statistic is of the form $\text{AIC}(\hat{\boldsymbol{\theta}}_0) - \text{AIC}(\hat{\boldsymbol{\theta}}) + 2k$ where k is the difference in the number of paremeters between the two models and $\text{AIC}(\hat{\boldsymbol{\theta}}_0)$ and $\text{AIC}(\hat{\boldsymbol{\theta}})$ are the AIC values of the Spatial+Seasonal and BI model, respectively. Since the BI model contains the Spatial+Seasonal model as a restricted case, the test statistic has an asymptotic χ^2_k distribution under the null hypothesis (Ogata, 1988). For these two models, the difference in parameters is 16 and the likelihood ratio test statistic has a value of 35.2, which is significant at the 5% level (p-value of 0.0037).

Figure 4 shows the estimated conditional intensity function for the BI model on the 15th of each month in 1999. The year 1999 is a typical year in the dataset, containing a total of 21 fires. For this year the intensity reaches its lowest point around March and generally increases through August. The conditional intensity is generally high in the northwest region of the County where much of the wildfire activity takes place.

5.1 Residual Analysis

While AIC is useful for determining the relative improvement of fit for competing models, one may be interested in a more refined analysis of a particular model. Residual analysis of the Spatial+Seasonal and BI models was conducted using both approximate random thinning and the rescaling method in order to identify possible departures of the models from the data

5.1.1 Approximate Thinned Residuals

For the approximate random thinning procedure we chose a subsample size of $K = 50$ for each thinning and generated 1000 thinnings from each model. Figure 5 shows the spatial coordinates for eight typical realizations of thinned residuals for the BI model. In each plot the residuals appear to be spread uniformly across the County. Recall that in Figure 1 the data were highly clustered in the northwest region near weather stations 1 and 2 and there were relatively few points in the northeast corner. The thinned residuals in Figure 5 appear to have corrected this imbalance somewhat.

Figure 6 shows the same thinned residuals but with the time and y-coordinates. Here we see a more interesting pattern. In many of the plots there is a cluster of points around the years 1979–1981, for instance in realizations number 5 and 8. In Section 3 it was noted that the original data had some increased activity in this same time period. The residual clustering indicates that the BI model is not adequately taking into account the clustering in the data around this specific time period. One possible explanation for this lack of fit is that the increased activity was not due to purely meteorological phenomena or changes in fuel properties. Indeed, the BI model for those years appears close to the Spatial+Seasonal model (this is discussed further in Section 5.1.2).

While visual inspection of the residuals can be a useful method of model evaluation, it

may be desirable to have a more systematic test available. Existing second-order methods for analyzing point patterns are largely two-dimensional, although there have been some extensions (e.g. Baddeley et al., 1993; Diggle et al., 1995). In order to test the homogeneity of the residual process, we used a space-time version of the K-function. The K-function evaluated at distance h is the proportion of pairs of points per unit area that are within distance h of each other. In order to evaluate the K-function, a distance function must be specified, which in spatial settings is typically Euclidean distance. For our application, we chose the following distance function, which is defined for two points (t_1, x_1, y_1) and (t_2, x_2, y_2) as

$$\text{Distance}\{(t_1, x_1, y_1), (t_2, x_2, y_2)\} = \sqrt{(x_1 - x_2)^2 + (y_1 - y_2)^2} + \delta|t_1 - t_2|$$

where δ is chosen so that the temporal and spatial scales are commensurate. Here this corresponds $\delta = 1/5475$ days, which sets a spatial distance of 5 miles roughly equivalent to a temporal distance of 4 years. Rather than plot the raw K-function, we use a normalized version of the L-function (Ripley, 1979) which is centered around zero for a homogeneous Poisson process.

Figure 7 shows the mean estimated L-functions for the 1000 approximate thinned residuals from both the Spatial+Seasonal model and the BI model. Note that the figure omits the negative range of the K-function. The estimated L-function for the BI model (solid black line) appears to decrease to zero faster than that of the Spatial+Seasonal model (gray line). However, there is significant clustering for smaller distances up to 1.0, which corresponds to about 18.9 miles in the spatial domain and 15 years in the temporal domain. This residual clustering indicates a lack of fit in the BI model. In the following section we explore further the temporal clustering in the residual process.

5.1.2 Rescaled Temporal Residuals

The fit of the BI model in the temporal domain can be assessed using the rescaling method (Meyer, 1971) to create a residual process on the line. Each original event time t_i $(i = 1, \ldots, n)$ is mapped to a new time

$$\tau_i = \int_{T_1}^{t_i} \iint_S \lambda(t, x, y; \hat{\boldsymbol{\theta}})\, dxdydt.$$

where T_1 is equal to January 1, 1976 and S is the spatial observation window. We can then check whether the residuals $\tau_1 < \cdots < \tau_n$ appear as a homogeneous Poisson process of rate 1 on the line. Figure 8(a) shows a histogram of the rescaled points and Figure 8(b) shows the empirical log-survivor function for the interevent times of the residual process. These plots exhibit two interesting phenomena. In Figure 8(a) we see that there are a very large number of points in the period 50–150 in transformed time. Since each histogram bin is of length 50, the number of points in each bin would be an i.i.d. Poisson random variable with mean and variance equal to 50 if the BI model fit perfectly. However, for the period 50–150 we observe 79 and 101 points in the two corresponding bins. On the original time scale the interval 50–150 corresponds approximately to the years 1978–1982. This result along with the clustering in the thinned residuals (observed in Figure 6) confirms that the increased wildfire activity during the years 1979–1981 is not captured by the BI model.

For a homogeneous Poisson process with rate 1, the interevent times have an exponential distribution with mean 1. In Figure 8(b) the distribution of the interevent times in the residual process seems to deviate considerably from exponential (dashed line). In particular, the tail of the distribution appears to be heavier than expected – the largest observation is more than 15 transformed time units.

The above mentioned anomalies can be examined with the original data to check for specific problems with the BI model. An entity that is of use in this task is the temporal

intensity function,

$$r(t) = \iint_S \lambda(t, x, y; \hat{\boldsymbol{\theta}})\, dxdy.$$

Figure 9 shows $r(t)$ over two different time intervals in the 25 year study period for the Spatial+Seasonal and BI model. Figure 9(a) shows $r(t)$ for the years 1979–1981, the period in which we observe an unusually high level of wildfire activity. If the BI were adequately representing the risk of fire due to severe weather, then one might expect the BI model to have a somewhat higher intensity during this time period, given the dependence of the BI on local weather and fuel properties. However, the BI model (gray line) appears to be quite close the Spatial+Seasonal model (black line) and significantly underestimates the rate of activity during these three years.

For comparison, Figure 9(b) shows the period 1990–1991, which contains the largest interevent time observed in Figure 8(b). The two vertical dotted lines indicate the two events which generated the large interevent time when rescaled. These two events correspond to the last fire in 1990 and the first fire in 1991. The first fire in 1991 comes on August 23rd, which is much later in the year than is typical for the first fire. Figure 9(b) shows that the BI model deviates considerably from the Spatial+Seasonal model. The estimated temporal intensity for the BI model is much lower than the Spatial+Seasonal model in the months between May and September. It seems that the BI model is reflecting a local change in weather or fuel conditions which is different from the usual seasonal pattern. However, it seems that the BI model is not compensating enough, thus creating the larger than expected interevent time. Nevertheless, Figure 9(b) illustrates a period of time where the BI model appears to be making a useful improvement over the Spatial+Seasonal model.

5.2 Model Predictions

Given a model for the conditional intensity of a point process, the process can be simulated via the random thinning algorithm of Lewis and Shedler (1979). We simulated one year's worth of events to see if features of the simulations matched those of the observed events. The BI model was re-fit using the wildfire and BI data from 1976 through 1998 and the Lewis-Shedler algorithm was applied to generate random realizations of wildfire events for 1999. The spatial distribution of the simulations (not shown) appeared to match the configuration of the observed fires fairly well. Figure 10 shows the the time and y-coordinates for eight typical simulations, where the "+" symbols represent the 21 fires actually observed in 1999. In Figure 10 we see that the BI model tends to predict more fires during the period between January and April than were actually observed. The first fire of 1999 was on January 3rd followed by a fire on April 23rd. However, in each simulation the BI model predicts some fires in the intervening months.

6 Summary and Discussion

In this article we have developed an approach for evaluating a wildfire hazard index using multi-dimensional point process models. This approach has allowed for a detailed analysis of the performance of the Burning Index in predicting wildfire occurrence in Los Angeles County. Our conclusions about the BI are based on an assessment of conditional intensity models which incorporate spatial, seasonal, and BI information. We find that the best-fitting model that incorporates BI information does not perform substantially better than a simple model which only takes into account natural spatial and seasonal variation.

Two point process residual analysis techniques were employed to supplement a standard likelihood based model evaluation criterion (AIC). Although the development and applica-

tion of residual methods for point processes is still an active area of research, their usefulness here has been clearly demonstrated. The random thinning method enabled us to check for residual space-time clustering on the same temporal and spatial scales as the data, while the rescaling method allowed for the closer inspection of temporal clustering in the residuals. Together, the methods provided insight into precisely where the BI model fit poorly and where it was making some (minimal) improvement.

In Section 5, we saw that the homogeneous Poisson model provides a rather poor fit to the data. This was expected, as the model does not take into account any spatial or seasonal variation and omits information about fuel and meteorological conditions. The BI model incorporates all of this information and clearly does much better than the homogeneous Poisson model. However, we found that the Spatial+Seasonal model (which does not contain any meteorological information) performs nearly as well as the BI model.

The values of the AIC indicate that the inclusion of BI information into the conditional intensity does improve the fit of the model to the data. However, both the residual analysis and the model predictions indicate that the BI model is far from adequate for predicting wildfire occurrence. In particular, we have identified two specific areas where the BI model provides a poor fit to the data. The first is the three year period between 1979 and 1981 and the second is the first quarter of 1999. Between 1979 and 1981 we observe an increased level of wildfire activity and the clustering in the thinned residuals during that time period indicates that the BI is doing little to account for this increased activity. In fact, the temporal intensity for the BI model tracks fairly closely the temporal intensity of the Spatial+Seasonal model for the entire three year period.

In Section 5.2 we saw that for 1999, a typical year, the BI model tends to overpredict in the months of January, February, and March. On average each of the simulations placed at least one fire in each of those months. The problem is that the BI values can in fact be high

during the winter. Figure 3 shows that on average many of the stations do not reach their lowest point until the middle of March or even April. Therefore, even though we do not observe many actual fires in January, February, and March, the BI model tends to produce a higher intensity because of the high BI values.

It is important to note the possible biases that may result from the missing data and the procedure used to fill in missing BI values. In Section 3 we replaced a missing value on a given day with the average of the non-missing values for that day across all years. If the non-missing values do not accurately represent the non-missing data, then the resulting estimated conditional intensity could be biased. In our initial examination of the BI data we found that stations with relatively low percentages of missing data had very regular seasonal patterns from year to year. While one would expect some natural variation between stations, we see no reason why the other stations should not exhibit the same strong seasonal patterns. Therefore, we feel that the biases resulting from the missing data are likely to be small. Determining the optimal use of station data, including developing methods for imputing missing values, is an important subject for future work.

Other possibilities for further investigation remain in both the areas of wildfire research and point processes. It may be of interest to wildfire researchers to examine the performance of other hazard indices in Los Angeles County, having already identified some specific deficiencies with the BI. In the area of point processes, the application of residual methods is still an active area of research. In particular, specific properties of thinned and rescaled residuals (and the behavior of corresponding test statistics) are not generally well known when model parameters have to be estimated (see e.g. Schoenberg, 2002). In addition, the development of visualization techniques and summary statistics for multi-dimensional point process data is an important topic for future research.

References

Albini, F. A. (1976), "Computer-based Models of Wildland Fire Behavior: A User's Manual," Tech. rep., USDA Forest Service, Intermountain Forest and Range Experiment Station.

Baddeley, A. J., Moyeed, R. A., Howard, C. V., and Boyde, A. (1993), "Analysis of a Three-dimensional Point Pattern with Replication," *Applied Statistics*, 42, 641–668.

Berman, M. (1983), "Comment on 'Likelihood Analysis of Point Processes and Its Applications to Seismological Data,' by Y. Ogata," *Bulletin of the International Statistical Institute*, 50, 412–418.

Bradshaw, L. S., Deeming, J. E., Burgan, R. E., and Cohen, J. D. (1983), "The 1978 National Fire-Danger Rating System: Technical Documentation," Tech. Rep. INT-169, USDA Forest Service, Intermountain Forest and Range Experiment Station.

Brémaud, P. M. (1981), *Point Processes and Queues: Martingale Dynamics*, Springer-Verlag, New York.

Brown, E. N., Barbieri, R., Ventura, V., Kass, R. E., and Frank, L. M. (2001), "The Time-Rescaling Theorem and its Application to Neural Spike Train Data Analysis," *Neural Computation*, 14, 325–346.

Burgan, R. E. (1988), "Revisions to the 1978 National Fire-Danger Rating System," Tech. Rep. SE-273, USDA Forest Service, Southeastern Forest Experiment Station.

Byram, G. M. (1959), "Combustion of Forest Fuels," in *Forest Fire Control and Use*, McGraw-Hill Book Co., New York.

Choi, E. and Hall, P. (1998), "Nonparametric Approach to Analysis of Space-Time Data on Earthquake Occurrences," *Journal of Computational and Graphical Statistics*, 8, 733–748.

Daley, D. J. and Vere-Jones, D. (2003), *An Introduction to the Theory of Point Processes: Volume I*, Springer, New York, 2nd ed.

Deeming, J. E., Burgan, R. E., and Cohen, J. D. (1977), "The National Fire-Danger Rating System — 1978," Tech. Rep. INT-39, USDA Forest Service, Intermountain Forest and Range Experiment Station.

Deeming, J. E., Lancaster, J. W., Fosberg, M. A., Furman, R. W., and Schroeder, M. J. (1972), "The National Fire-Danger Rating System," Tech. Rep. RM-84, USDA Forest Service, Rocky Mountain Forest and Range Experiment Station.

Diggle, P. J. (1983), *Statistical Analysis of Spatial Point Patterns*, Academic Press, NY, London.

— (1990), "A Point Process Modelling Approach to Raised Incidence of a Rare Phenomenon in the Vicinity of a Prespecified Point," *Journal of the Royal Statistical Society, Series A*, 153, 349–362.

Diggle, P. J., Chetwynd, A. G., Häggkvist, R., and Morris, S. E. (1995), "Second-order Analysis of Space-Time Clustering," *Statistical Methods in Medical Research*, 4, 124–136.

Haines, D. A., Main, W. A., Frost, J. S., and Simard, A. J. (1983), "Fire-Danger Rating and Wildfire Occurrence in the Northeastern United States," *Forest Science*, 29, 679–696.

Jacod, J. (1975), "Multivariate Point Processes: Predictable Projection, Radon-Nikodym Derivatives, Representation of Martingales," *Zeitschrift für Wahrscheinlichkeitstheorie und Verwandte Gebiete*, 31, 235–253.

Lewis, P. A. W. and Shedler, G. S. (1979), "Simulation of Nonhomogeneous Poisson Processes by Thinning," *Naval Research Logistics Quarterly*, 26, 403–413.

Mandallaz, D. and Ye, R. (1997), "Prediction of Forest Fires with Poisson Models," *Canadian Journal of Forest Research*, 27, 1685–1674.

Merzbach, E. and Nualart, D. (1986), "A Characterization of the Spatial Poisson Process and Changing Time," *Annals of Probability*, 14, 1380–1390.

Meyer, P. (1971), "Demonstration Simplefiée d'un Théorème de Knight," in *Séminaire de Probabilités* ***V***, Université Strasbourg, vol. 191 of *Lecture Notes in Mathematics*, pp. 191–195.

Nair, M. G. (1990), "Random Space Change for Multiparameter Point Processes," *Annals of Probability*, 18, 1222–1231.

Ogata, Y. (1978), "The Asymptotic Behavior of Maximum Likelihood Estimators for Stationary Point Processes," *Annals of the Institute of Statistical Mathematics*, 30, 243–261.

— (1981), "On Lewis' Simulation Method for Point Processes," *IEEE Transactions on Information Theory*, 27, 23–31.

— (1988), "Statistical Models for Earthquake Occurrences and Residual Analysis for Point Processes," *Journal of the American Statistical Association*, 83, 9–27.

Ogata, Y. and Akaike, H. (1982), "On Linear Intensity Models for Mixed Doubly Stochastic Poisson and Self-exciting Point Processes," *Journal of the Royal Statistical Society, Series B*, 44, 102–107.

Ogata, Y., Akaike, H., and Katsura, K. (1982), "The Application of Linear Intensity Models to the Investigation of Causal Relations between a Point Process and Another Stochastic Process," *Annals of the Institute of Statistical Mathematics*, 34, 373–387.

Rathbun, S. L. (1993), "Modeling Marked Spatio-temporal Point Patterns," *Bulletin of the International Statistics Institute*, 55, 379–396.

— (1996), "Asymptotic Properties of the Maximum Likelihood Estimator for Spatio-temporal Point Processes," *Journal of Statistical Planning and Inference*, 51, 55–74.

Rathbun, S. L. and Cressie, N. (1994), "Asymptotic Properties of Estimators for the Parameters of Spatial Inhomogeneous Poisson Point Processes," *Advances in Applied Probability*, 26, 122–154.

Ripley, B. D. (1979), "Tests of 'Randomness' for Spatial Point Patterns," *Journal of the Royal Statistical Society, Series B*, 41, 368–374.

— (1981), *Spatial Statistics*, Wiley, New York.

Rothermel, R. C. (1972), "A Mathematical Model for Predicting Fire Spread in Wildland Fuels," Tech. Rep. INT-115, USDA Forest Service.

Schoenberg, F. (1997), "Assessment of Multi-dimensional Point Process Models," Ph.D. thesis, University of California, Berkeley.

— (1999), "Transforming Spatial Point Processes into Poisson Processes," *Stochastic Processes and their Applications*, 81(2), 155–164.

Schoenberg, F. P. (2002), "On Rescaled Poisson Processes and the Brownian Bridge," *Annals of the Institute of Statistical Mathematics*, 54, 445–457.

— (2003), "Multi-dimensional Residual Analysis of Point Process Models for Earthquake Occurrences," Tech. Rep. 347, University of California, Los Angeles.

Schoenberg, F. P., Brillinger, D. R., and Guttorp, P. M. (2002), "Point Processes, Spatial-

Temporal," in *Encyclopedia of Environmetrics*, eds. El-Shaarawi, A. and Piegorsch, W., Wiley, NY, vol. 3, pp. 1573–1577.

Schoenberg, F. P., Peng, R., Huang, Z., and Rundel, P. (2003a), "Detection of Nonlinearities in the Dependence of Burn Area on Fuel Age and Climatic Variables," *International Journal of Wildland Fire*, in press.

Schoenberg, F. P., Peng, R., and Woods, J. (2003b), "On the Distribution of Wildfire Sizes," *Environmetrics*, in press.

Viegas, D. X., Bovio, G., Ferreira, A., Nosenzo, A., and Sol, B. (1999), "Comparative Study of Various Methods of Fire Danger Evaluation in Southern Europe," *International Journal of Wildland Fire*, 9, 235–246.

Warren, J. R. and Vance, D. L. (1981), "Remote Automatic Weather Station for Resource and Fire Management Agencies," Tech. Rep. INT-116, USDA Forest Service, Intermountain Forest and Range Experiment Station.

Westerling, A. L., Cayan, D. R., Gershunov, A., Dettinger, M. D., and Brown, T. (2000), "Western Wildfire Season Forcast," `http://meteora.ucsd.edu/cap/fire_forecast.html`.

Zhuang, J., Ogata, Y., and Vere-Jones, D. (2002), "Stochastic Declustering of Space-Time Earthquake Occurrences," *Journal of the American Statistical Association*, 97, 369–380.

A Tables

Station #	1	2	3	4	5	6	7	8
Jan–Apr	99.8	49.2	34.3	60.8	33.3	32.5	23.3	26.1
May–Dec	46.4	36.3	17.8	32.0	14.5	18.6	6.7	14.2
Overall	64.0	40.5	23.2	41.5	20.7	23.2	12.2	18.1

Table 1: Percentage of missing values for each weather station during the off-season (Jan–Apr), the fire season (May–Dec), and overall.

Model	$\hat{\mu}$	$\hat{\nu}$	$\hat{\phi}_x$	$\hat{\phi}_y$	$\hat{\alpha}$	$\hat{\phi}_{\text{seas}}$
H. Poisson	0.0041					
Spatial+Seasonal		0.0348	0.0440	0.0259	0.7053	8.44
BI model		0.0293	0.0339	0.0200	0.5570	8.27

Table 2: Maximum likelihood estimates of parameters for non-BI components. "H. Poisson" refers to the homogeneous Poisson model in (1).

	$s = 1$	2	3	4	5	6	7	8
$\hat{\gamma}_s$ ($\times 10^{-5}$)	2.2	0.0	0.0	17.4	3.1	0.0	25.6	0.0
$\hat{\beta}_s$	0.001	3.000	3.000	0.387	0.001	0.442	0.520	0.816

Table 3: Maximum likelihood estimates for parameters in the BI component.

B Figure Captions

1. Spatial distribution of wildfires larger than 10 acres in Los Angeles County (1976–2000). Locations of the 8 Remote Automatic Weather Stations in Los Angeles County are indicated by the numbers above the solid cirlces. One spatial unit is approximately 18.9 miles.

2. Dates of occurrence and areas burned for fires larger than 10 acres (1976–2000).

3. Average yearly BI pattern.

4. Estimated conditional intensity function for the BI model on the 15th of each month in 1999. The units are in events / (spatial unit^2 $\times$ day) where one spatial unit is approximately 18.9 miles.

5. Eight random realizations of thinned residuals for the BI model (spatial coordinates).

6. Residuals for the BI model (time and y-coordinate).

7. Normalized K-function for the Spatial+Seasonal (solid gray line) and BI (solid black line) models. The dotted line is the upper 95th percentile (pointwise) for the K-function applied to 1000 realizations of a homogeneous Poisson process.

8. (a) Histogram of the rescaled residual process; (b) Log-survivor plot of the interevent times for the rescaled residual process. The dashed line represents the theoretical log-survivor function for the exponential distribution.

9. Temporal intensity functions $r(t)$ for the Spatial+Seasonal (black line) and BI model (gray line) for (a) 1979–1981; and (b) 1990–1991.

10. Simulations from the BI model ("o") and observed wildfires ("+") for the year 1999.

C Figures

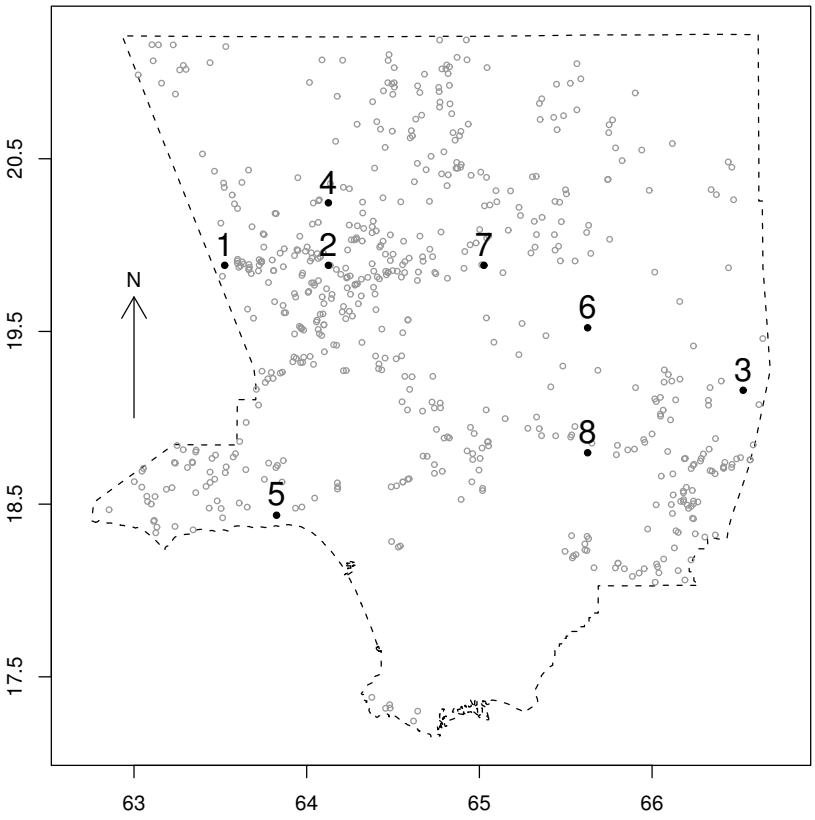

Figure 1: Spatial distribution of wildfires larger than 10 acres in Los Angeles County (1976–2000). Locations of the 8 Remote Automatic Weather Stations in Los Angeles County are indicated by the numbers above the solid cirlces. One spatial unit is approximately 18.9 miles.

Figure 2: Dates of occurrence and areas burned for fires larger than 10 acres (1976–2000).

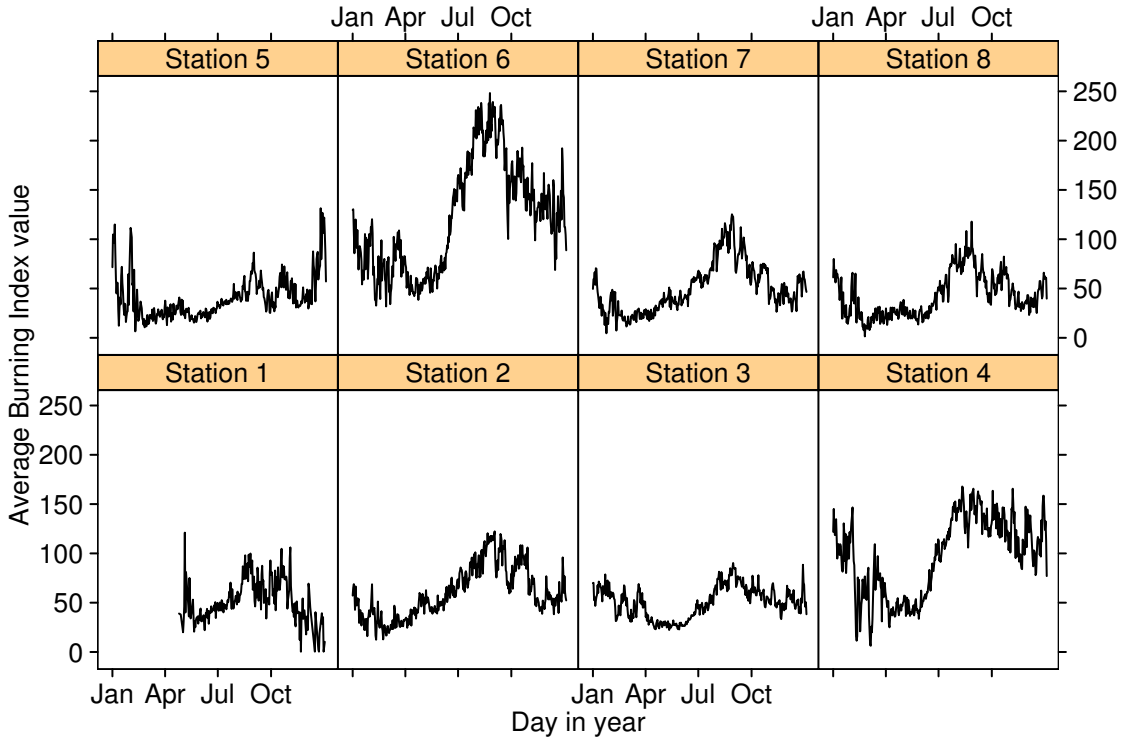

Figure 3: Average yearly BI pattern.

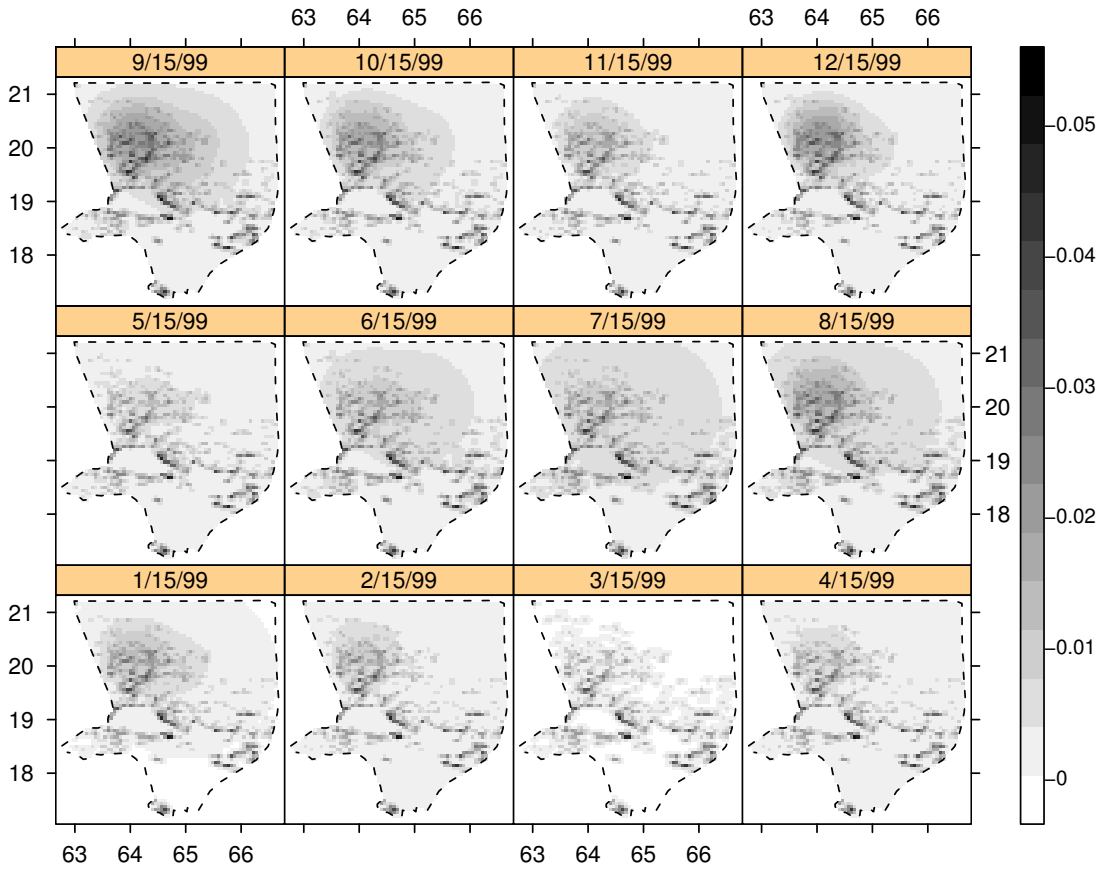

Figure 4: Estimated conditional intensity function for the BI model on the 15th of each month in 1999. The units are in events / (spatial unit^2 $\times$ day) where one spatial unit is approximately 18.9 miles.

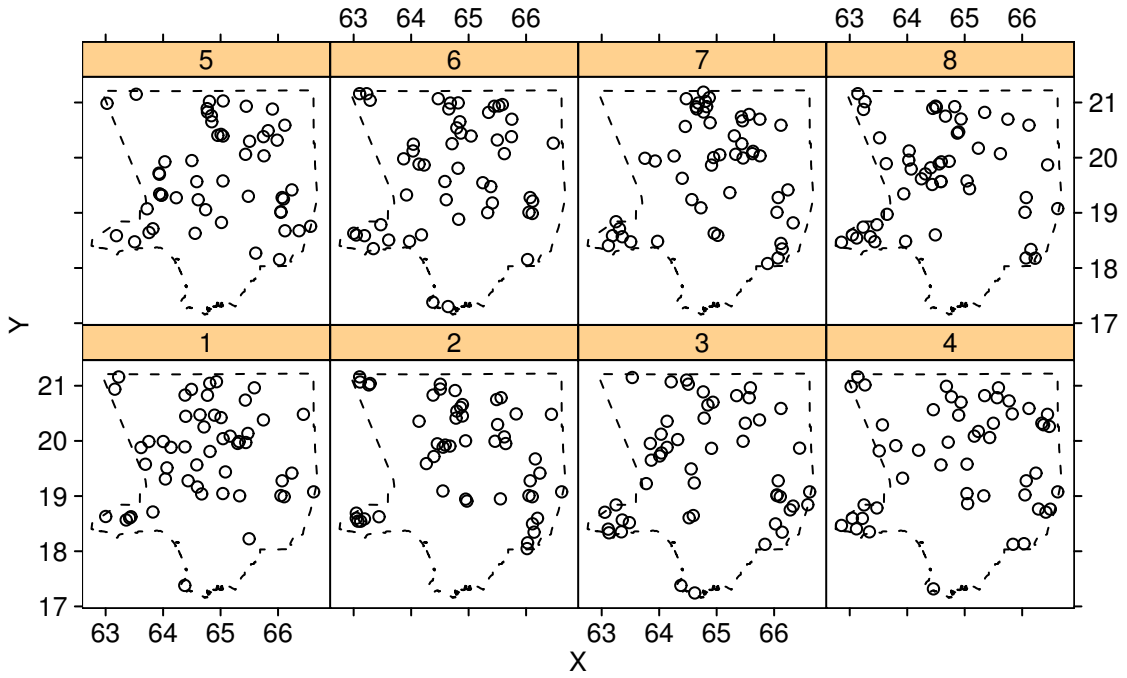

Figure 5: Eight random realizations of thinned residuals for the BI model (spatial coordinates).

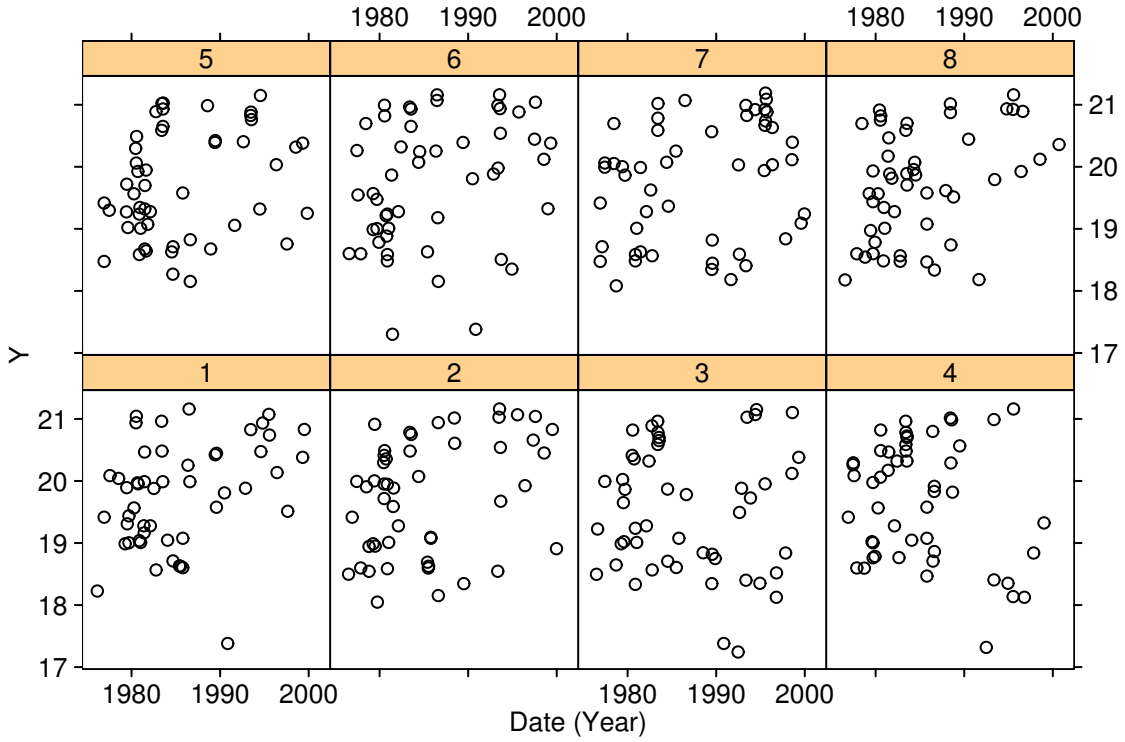

Figure 6: Residuals for the BI model (time and y-coordinate).

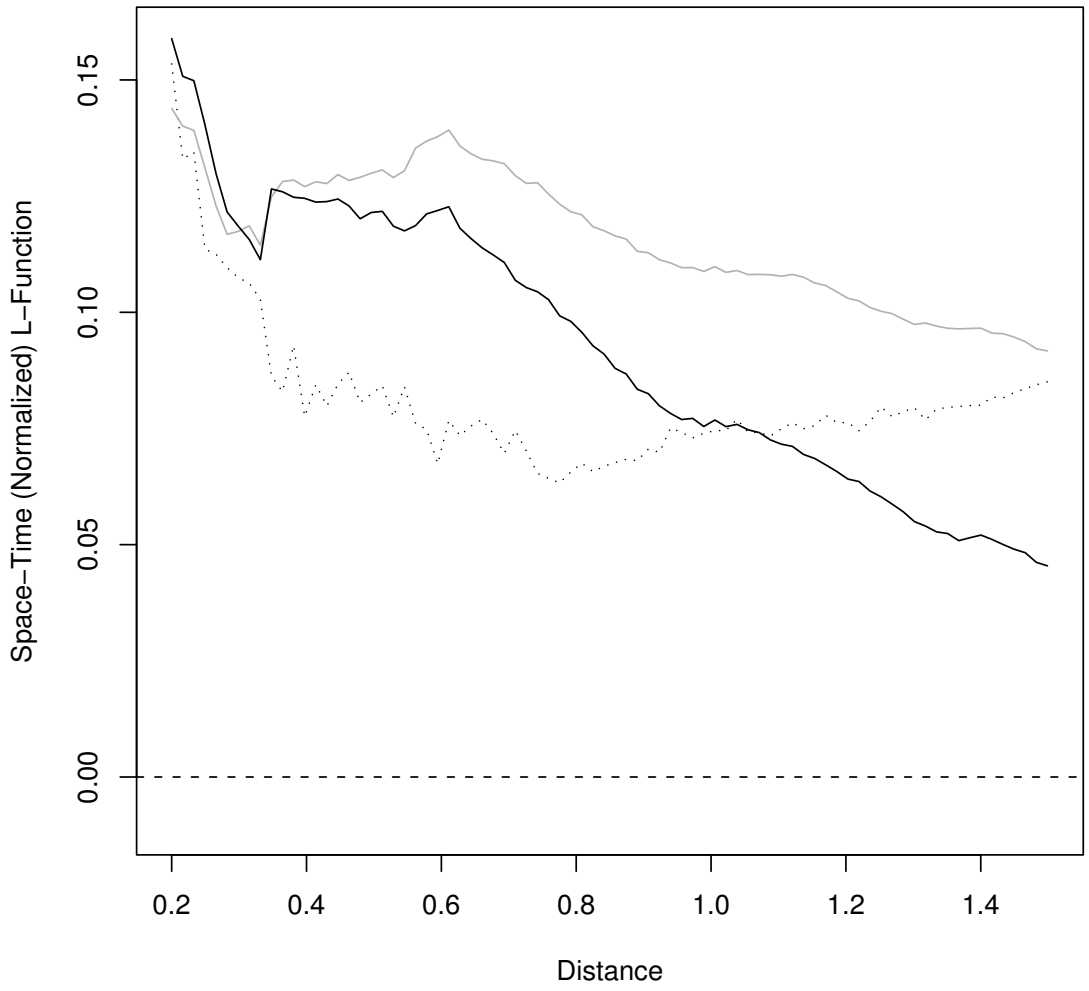

Figure 7: Normalized K-function for the Spatial+Seasonal (solid gray line) and BI (solid black line) models. The dotted line is the upper 95th percentile (pointwise) for the K-function applied to 1000 realizations of a homogeneous Poisson process.

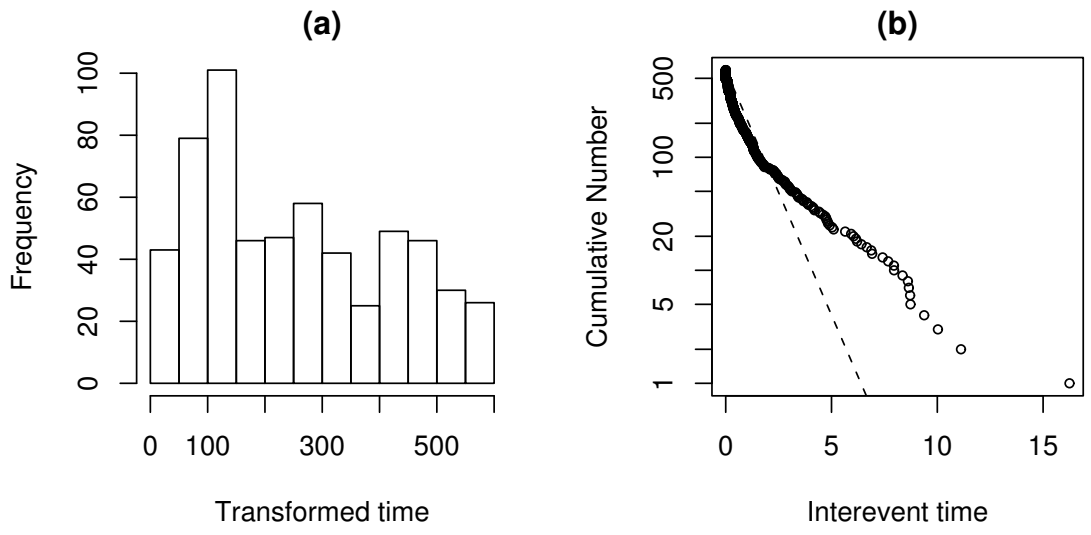

Figure 8: (a) Histogram of the rescaled residual process; (b) Log-survivor plot of the interevent times for the rescaled residual process. The dashed line represents the theoretical log-survivor function for the exponential distribution.

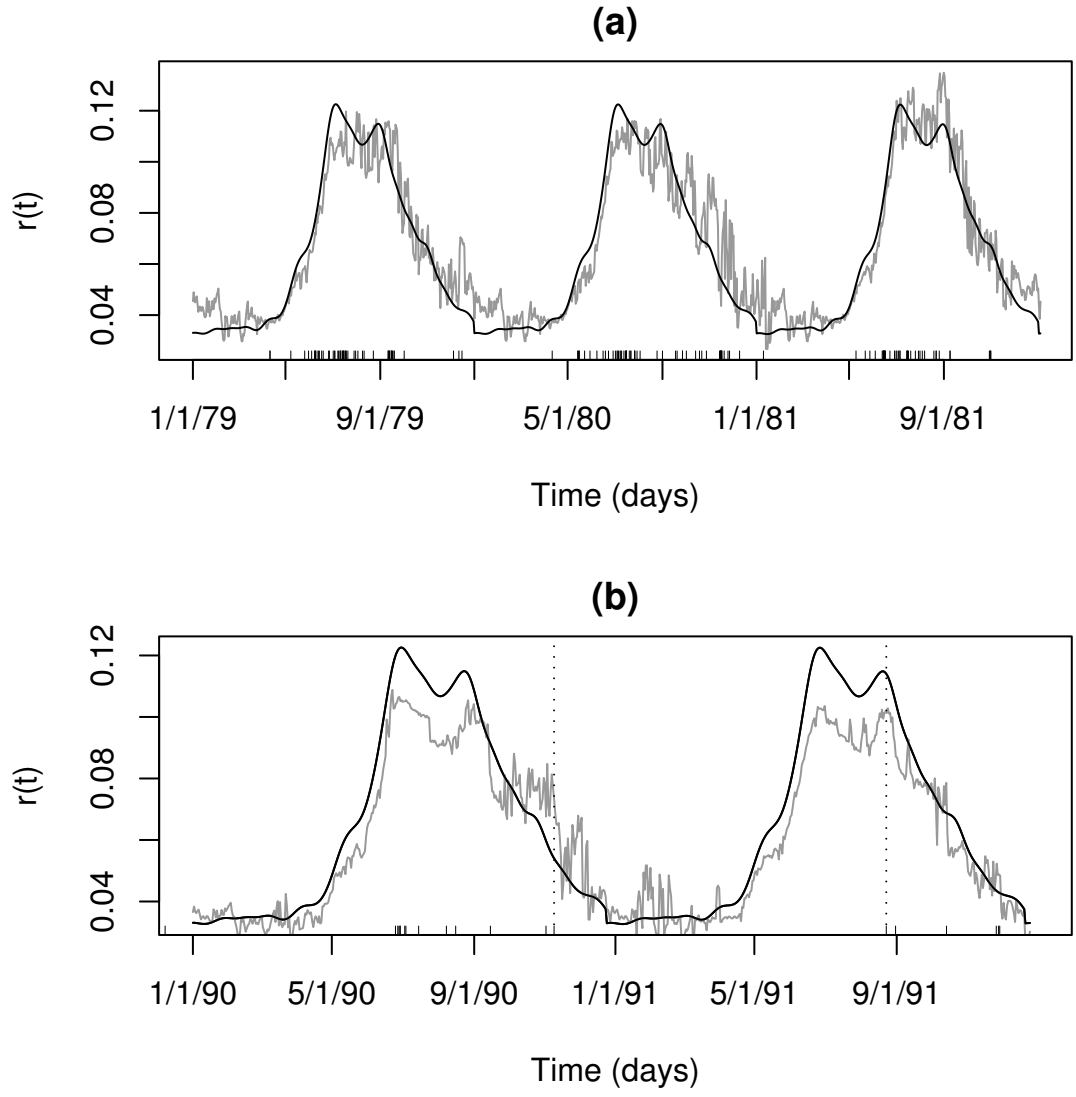

Figure 9: Temporal intensity functions $r(t)$ for the Spatial+Seasonal (black line) and BI model (gray line) for (a) 1979–1981; and (b) 1990–1991.

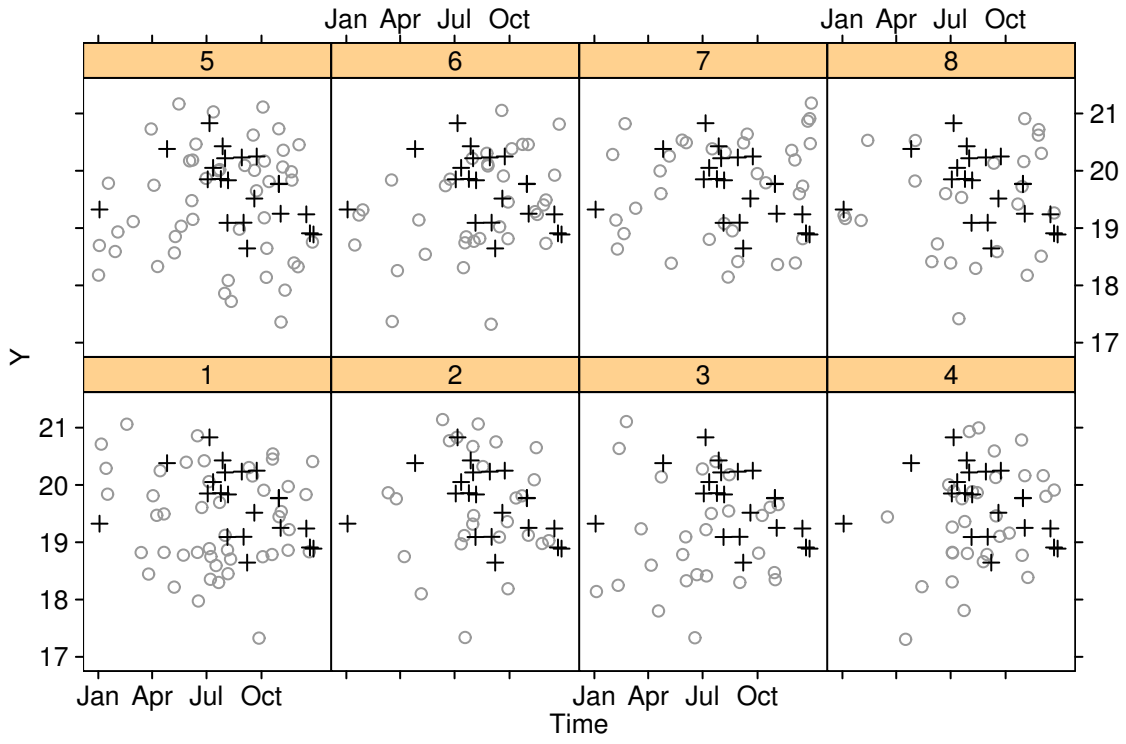

Figure 10: Simulations from the BI model ("o") and observed wildfires ("+") for the year 1999.